

Chip Scale Atomic Clocks: current status and future prospects

Tommaso Bocchietti

April 11, 2024

UNIVERSITY OF
WATERLOO



Abstract

Chip-Scale Atomic Clocks (CSACs) can be considered as one of the most significant advancements in timekeeping technology considering their low power consumption, small size, and high stability and accuracy in frequency. Originally developed for military purposes, CSACs have found applications in various fields where accurate timekeeping and portability are essentials, such as satellite navigation, oil industry exploration, telecommunications, and space experimental physics.

This report will provide an overview of the key parameters, discuss the governing physics highlighting the bottleneck and limitations, and explore their current and potential applications across different sectors. A final section will focus on the future prospects and challenges in the development of the next generation of CSAC technology.



Figure 1: Microsemi SA.65 Chip Scale Atomic Clock, the most advanced CSAC commercially available since 2021. Source: [26].

Contents

1	Introduction	5
2	Objective metrics for timekeeping devices	5
2.1	Definition of the Second [s]	5
2.2	Stability	5
2.2.1	Short-term stability	6
2.2.2	Medium-term stability	7
2.2.3	Long-term stability	7
2.3	Other metrics	7
3	Working Principles	8
3.1	General overview of a CSAC	8
3.2	Physics Package (PP)	9
3.2.1	Microwave Optical Double-Resonance (MODR)	9
3.2.2	Coherent Population Trapping (CPT)	12
3.3	Control Loop (CL)	18
3.4	Local Oscillator (LO)	20
4	Performances and Limitations	20
4.1	Short-term frequency stability	21
4.2	Medium-term frequency stability	21
4.3	Long-term frequency stability	23
4.4	Frequency Stability vs. Size, Weight, and Power (SWaP)	23
5	Applications	24
5.1	Global Navigation Satellite System (GNSS)	24
5.2	Military Applications	25
5.3	Ocean Bottom Seismics (OBS)	26
5.4	Other Applications	26
6	Future prospects	27
6.1	Motivations for Next Generation CSACs	27
6.2	Proposed research directions	28
6.2.1	Microwave transitions in laser-cooled alkali metals	28
6.2.2	Microwave transitions in double-resonance trapped ions	28
6.2.3	Optical transitions in warm atomic/molecular vapors	29
7	Conclusion	29
A	Atomic clock extensive comparison	33
B	Chip-Scale Atomic Clocks comparison	34
C	Rubidium energy levels	35
D	Cesium energy levels	36

List of Figures

1	Microsemi SA.65 Chip Scale Atomic Clock, the most advanced CSAC commercially available since 2021. Source: [26].	2
2	Overall stability of a clock source as summation of the different contributions from the internal components and processes. Observing the overall stability (red line), we can distinguish three main regions: short-term ($0 \leq \tau \leq 10^0 s$), medium-term ($10^0 \leq \tau \leq 10^3 s$), and long-term (beyond the flicker floor). Source [20].	6
3	General overview of a CSAC	9
4	MODR-based CSAC scheme. Source [19].	10
5	Population inversion and decay.	11
6	Microwave excitation.	11
7	Optical interrogation.	11
8	Electrons cycle in a MODR-based CSAC due to the optical pumping, microwave excitation, and optical interrogation.	11
9	CPT-based CSAC scheme. Source [19].	13
10	Ground state.	14
11	Superposition state.	14
12	Excited state.	14
13	State superposition via Bloch sphere representation.	14
14	State superposition via modal interpretation and wave functions.	14
15	Λ -system representation. Source [25].	15
16	Beating wave of the laser source in a CPT-based CSAC (AM modulation is highlighted with a dashed gray line, FM modulation is clearly visible on the green wave).	16
17	Population inversion.	17
18	Population decay.	17
19	Optical interrogation.	17
20	Electrons cycle in a CPT-based CSAC due to the optical pumping, decay and optical interrogation.	17
21	Detuned photodetection signal in a CPT-based CSAC. Source [19].	18
22	Control Loops block diagram for a CPT-based architecture (note the presence of the VCSEL). Source [20].	18
23	Allan deviation plot $\sigma_y(\tau)$ for different clock type sources (Cesium (Cs) Beam Standard , Rubidium (Rb) vapor cell clock , Oven-controlled crystal oscillator (OCXO) , Temperature-compensated crystal oscillator (TCXO)). Source [20].	21
24	Allan deviation $\sigma_y(\tau = 1s)$ vs. Size, Weight, and Power (SWaP) for different atomic clocks. Source [11].	24
25	Stability targets for the DARPA IMPACT and ACES programs. Source [23].	27
26	Energy levels of ^{87}Rb . Source [37].	35
27	Energy levels of ^{87}Rb . Source [37].	36

List of Tables

1	Performance parameter for some of the most common atomic clock. Source [23].	33
2	Key parameters of the most common CSACs. Source [38].	34

1 Introduction

The importance of precise timekeeping Accurate timekeeping has always been essential for human activities, from coordinating daily tasks to enabling global communication and navigation systems. Over time, scientists have developed increasingly precise timekeeping devices, with the invention of atomic clocks marking a significant advancement in this field and setting new standards for accuracy and stability.

However, traditional atomic clocks are large, complex, and power-hungry devices, limiting their portability and widespread use.

The exigence of miniaturization In the early 2000s, the need for an ultra-miniaturized, low-power atomic time and frequency reference unit arose, driven by military exigences from the Defense Advanced Research Projects Agency. DARPA collaborated with the National Institute of Standards and Technology (NIST) to develop the first working prototype of Chip-Scale Atomic Clock (CSAC) in 2004, which was a milestone achievement in atomic clock technology.

Current uses and future potential Leveraging the natural oscillations of atoms, CSACs are able to achieve frequency stability on the order of 10^{-10} over one second time period while consuming less than 120mW of power and fitting into a total volume of less than 17cm^3 . These remarkable performance metrics have enabled CSACs to find applications in a wide range of fields, where precise timekeeping over short periods of time is essential. Moreover, the compact size and low power consumption of CSACs make them ideal for integration into portable devices or in systems where space and power are limited.

In this paper, we will try to understand the main concepts behind the operation of CSACs, what are the current limitations, and what we can expect from the future development of this technology.

2 Objective metrics for timekeeping devices

Before diving into the core subject of CSACs, it's important to give some definitions and explain the key parameters that define the performance of these devices. Those parameters will be used in Section 4 as objective metrics to compare and highlight the major differences between various architecture of the clocks.

2.1 Definition of the Second [s]

The Bureau International des Poids et Mesures (BIPM), which is one of the three organizations that define the International System of Units (SI), defines the Second as: *the fixed numerical value of the Cs frequency $\Delta\nu_{Cs}$, the unperturbed ground-state hyperfine transition frequency of the ^{133}Cs atom, to be $9.192.631.770$ when expressed in the unit Hz, which is equal to s^{-1} .*

This kind of definition was first adopted starting from the year 1967, when experimental work showed the accuracy and reproducibility of transition between two energy levels of an atom or a molecule. The current definition was proposed and adopted starting from 2018, and it's also the basis of modern atomic clocks.

2.2 Stability

Stability, when referring to a clock source, is the measure of how well the reference frequency can be maintained over time. All the metrics used to define the stability of a clock are based on

the fractional frequency error, which is the ratio between the frequency error and the reference frequency, namely:

$$y(t) = \frac{f(t) - f_0}{f_0} \quad (1)$$

Where $f(t)$ is the frequency of the clock at time t , and f_0 is the nominal frequency of the clock. In the framework of CSACs, or more in general of atomic clocks, three main regions can be identified in the stability plot: short-term, medium-term, and long-term stability.

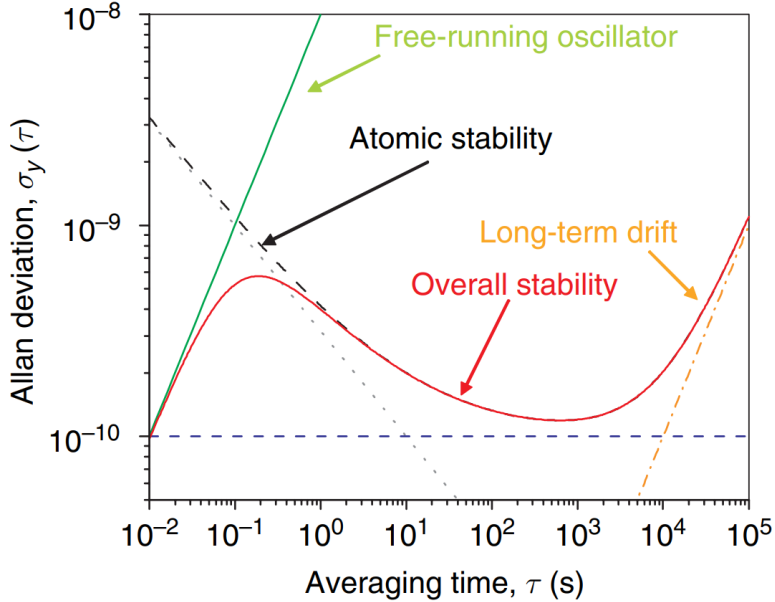


Figure 2: Overall stability of a clock source as summation of the different contributions from the internal components and processes. Observing the overall stability (red line), we can distinguish three main regions: short-term ($0 \leq \tau \leq 10^0 s$), medium-term ($10^0 \leq \tau \leq 10^3 s$), and long-term (beyond the flicker floor). Source [20].

2.2.1 Short-term stability

Short-term stability refers to the performance of a clock over very short time intervals, typically ranging from a few milliseconds to a few seconds. Allan deviation (denoted as $\sigma_y(\tau)$) is the metric used to measure it, capturing both rapid fluctuations (Fast Noise) and gradual drifts (Slow Drift) in the output frequency. From its definition, Allan deviation (ADEV) can be computed as:

$$\sigma_y(\tau) = \sqrt{\frac{1}{2M} \sum_{i=2}^M (\bar{y}(\tau)_i - \bar{y}(\tau)_{i-1})^2} \quad (2)$$

Where $\bar{y}(\tau)_i$ is the average fractional frequency error over the time interval τ and M is the number of sampling data.

To give a more practical example, we can consider a clock running with an output frequency of $f_0 = 10 MHz$, having an Allan deviation of $\sigma_y(\tau = 1s) = 3 \times 10^{-9}$. In this case, the instability in frequency between two observations 1 second apart has an RMS value of 3×10^{-9} , that means a $10 MHz * 3 \times 10^{-9} = 30 mHz$ RMS¹ movement in frequency mostly due to the Fast Noise. As we will see in Section 4, for a CSAC clock the component having a major impact on the Fast Noise is the Local Oscillator (LO).

¹RMS: Room Mean Square

2.2.2 Medium-term stability

Medium-term stability refers to the performance of a clock over longer time intervals, typically ranging from a few seconds to a few minutes or hours. Allan deviation is again the metric used to measure it. In this case however, ADEV can be computed using an approximated version of Equation 2:

$$\sigma_y(\tau) = \frac{1}{Q \times SNR} \tau^{-1/2} \quad (3)$$

Where $Q = \frac{\nu_0}{\Delta\nu}$ and $SNR = \frac{P_{signal}}{P_{noise}}$ are related to the quality of the output signal in terms of frequency and power.

This simplified version of the Allan deviation can be adopted knowing that Fast Noise is no longer the main source of instability, and the Slow Drift becomes the dominant factor.

As we will see in Section 4, for a CSACs clock, the cause of the medium-term stability cannot be brought back to a single component, but it's the result of multiple and concurrent effects.

2.2.3 Long-term stability

Long-term stability refers to the performance of a clock over very long time intervals, typically ranging from a few days to a few years. Fractional frequency error is the metric used to measure this, and it's computed from the definition given in Equation 1.

It's common to consider as the starting point from which consider long-term stability region, the flicker floor. On a $\sigma_y(\tau)$ plot, the flicker floor can be identified as the point where the Allan deviation reaches a minimum value and then starts to increase again.

At such long time scale, multiple factors influence this metric as for example aging, environmental conditions, and other external factors. The summation of all these factors is usually referred to as Drift.

2.3 Other metrics

While stability is probably the most important parameter to define the performance of a clock, other metrics are also used to give a more complete overview of the device. Some of the most important ones are:

- Phase noise $\mathcal{L}(f)$: represents the noise power relative to the carrier contained in a 1 Hz bandwidth centered at a certain offset from the carrier. It's typically expressed in units of dBc/Hz .
- Temperature sensitivity *tempco*: measures how much the clock's performance varies with temperature changes. It's typically expressed in units of $ppb/^\circ C$.
- Operating temperature range: defines the minimum and maximum temperatures the clock can function within.

In the following sections, we will focus mainly on the stability, power consumption, and size of the CSAC, given that the original purpose of this technology was to create a reliable, portable and low-power atomic clock.

3 Working Principles

Chip-Scale Atomic Clocks (CSACs) can be divided into two main categories based on the atomic element they use and the operating principle they follow. In this section, we will explore and highlight the key components and contrasting approaches of these two families of CSACs, namely:

- Microwave Optical Double-Resonance (MODR), based on Rubidium (Rb)
- Coherent Population Trapping (CPT), based on Cesium (Cs)

As we will see, the two technologies have analogous structures, but they differ in the physics package, which is the core of the clock.

3.1 General overview of a CSAC

Before proceeding analyzing in detail the components of a CSAC, it's important to understand the general idea that governs its operation.

With respect to traditional quartz oscillators, CSACs exploit the use of a close loop control system to stabilize the frequency of the local oscillator to the atomic transition frequency. In other words, CSACs leverage the intrinsic stability of atomic transitions to discipline an oscillating circuit based on a vibrating quartz crystal. Many of the instabilities that affect traditional oscillators, such as temperature sensitivity, aging, and vibration sensitivity (common in classical quartz oscillators), are mitigated by relying on atomic transitions that by their nature are more stable and less sensitive to external factors.

The Building Blocks From a functional perspective, a CSAC can be broken down into three main blocks, each with a specific role in the system:

- Physics Package (PP): it can be considered the heart of the clock. It contains a vapor cell where the atomic excitation and interrogation take place.
- Control Loop (CL): it can be considered the brain of the clock. It constantly analyzes signals from the physics package and uses this information to fine-tune the frequency of the local oscillator.
- Local Oscillator (LO): it's the effective source of the clock. Given its intrinsic instabilities, it's constantly disciplined by the control loop to lock its frequency to a known multiple of the atomic transition frequency.

Notice that a fourth block is also present in the system, that is the Frequency Synthesizer (FS), which takes the LO's frequency and multiplies it by a known factor to match the range of frequencies needed to interact with the atoms within the physics package. For the sake of simplicity, we will not delve into the details of the FS in this section, limiting our analysis to the PP, CL, and LO.

The mentioned components are arranged in a closed-loop system, as illustrated in Figure 3.

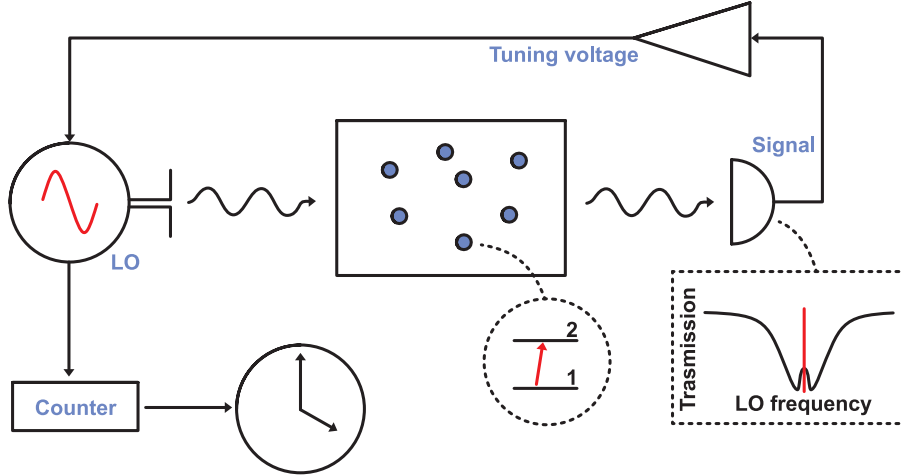


Figure 3: General overview of a CSAC

In the following sections, we will go through each main block of the CSAC, highlighting their fundamental physics and explaining their role in the general framework of the clock. In Section 4, all the limitations and bottleneck associated to each components will be discussed, analyzing their impact on the overall performance of the clock.

3.2 Physics Package (PP)

The Physics Package (PP) is the core component of the CSAC, where the atomic excitation and interrogation take place.

Its function is to compare the frequency of the local oscillator with the atomic transition frequency and generate a signal that measures the difference between the two. From a logical point of view, a generic PP receive as input the local oscillator frequency, and generate as output an electric signal that is sent to the control loop. Electric power to excite the atoms and thermal power to maintain a steady temperature are also provided to the PP to ensure proper operation.

One of the keys in the stability of a CSAC, lies in the capacity of the PP to generate a stable and accurate source of energy required for the excitation of the atoms, which leads to a stable and accurate signal for the control loop.

As we have mentioned at the beginning of this section (Section 3), CSACs can be divided into two main families based on the atomic element they use and the operating principle they follow. In the following subsections (Subsections 3.2.1 & 3.2.2), we will delve into the specific architecture for the PP of the two main families of CSACs, namely the one based on Microwave Optical Double-Resonance (MODR) and the one based on Coherent Population Trapping (CPT).

3.2.1 Microwave Optical Double-Resonance (MODR)

In a PP based on Microwave Optical Double-Resonance (MODR), a vapor gas cell is irradiated simultaneously by a microwave signal (coming from the local oscillator) and a high frequency signal (coming from a laser source). The combination of the two acting on the Rubidium (Rb) atoms inside the cell allows understanding whether the local oscillator is in resonance with the atomic transition frequency or not.

In order to better visualize the operation of a MODR-based CSAC, we leave here a schematic representation of its PP (Figure 4).

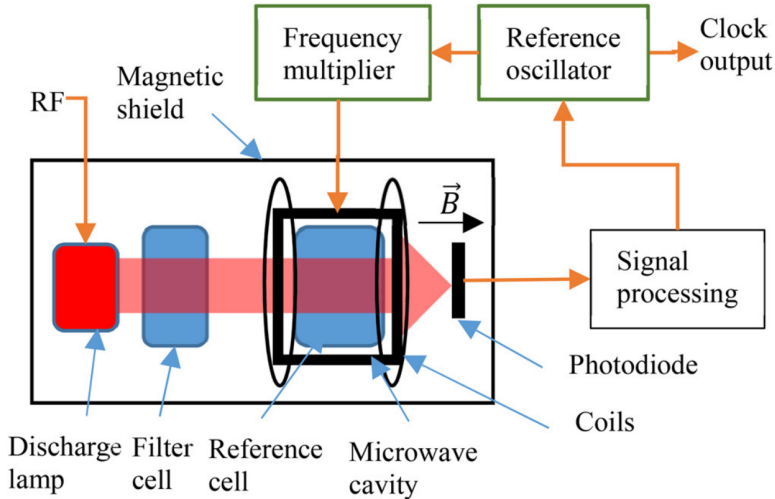


Figure 4: MODR-based CSAC scheme. Source [19].

Target Electron Transitions of Rubidium (Rb) In case of PP based on MODR, the vapor gas cell (also called reference cell) is typically filled with Rubidium (Rb) (^{87}Rb) atoms. Rb is an alkaline metal with a relatively simple electronic structure, defined as $[\text{Kr}]5s^1$. Its first ionization energy is 4.177eV , and the valence electron can be excited using relatively low energy photons. For these reasons, Rb is widely used in atomic clocks, as it allows for precise manipulation of the valence electron while containing the energy required for the excitation. In particular, by recalling the quantum energy levels of ^{87}Rb (defined by quantum effects and interactions between the electron and the nucleus), we can better define our working frame for the MODR architecture. Three different transitions are of interest regarding the ^{87}Rb atom²:

$$\text{Rb.I } 5^2S_{1/2} \quad F = 1 \rightarrow 5^2S_{1/2} \quad F = 2: \approx 6.8\text{GHz}$$

$$\text{Rb.II } 5^2S_{1/2} \quad F = 1 \rightarrow 5^2P_{1/2}: \approx 795^{-}\text{nm}$$

$$\text{Rb.III } 5^2S_{1/2} \quad F = 2 \rightarrow 5^2P_{1/2}: \approx 795^{+}\text{nm}$$

Notice that the transition $5^2S_{1/2} \rightarrow 5^2P_{1/2}$, of $\approx 795\text{nm}$, is usually refereed to as *D1 line*. As we will see in the following paragraphs, the only transitions that will excite the atoms in the reference cell are Rb.I and Rb.II. Transition Rb.III is in fact a non-targeted transition that will be filtered out by the system before reaching the reference cell.

Pumping Source Having defined our working frame in terms of electron transitions of ^{87}Rb , we can now step into understanding the mechanism used to excite the atoms in the reference cell.

In a MODR-based CSAC, the pumping source is typically a *bulb lamp* (also refereed to as *discharge lamp*, see Figure 4) containing ^{87}Rb atoms that after being excited to a higher energy level by an external power source, they decay back to the ground energy level emitting photons. Since there is no control over the pumping process inside the bulb lamp, more than one transition can be excited. This means that the lamp will emit photons corresponding to different transitions of the ^{87}Rb atoms, including among the others Rb.II and Rb.III transitions. However, the photons coming from the Rb.III transition are not of interest for the operation of the CSAC, and they need to be filtered out. To do so, a filter cell of ^{85}Rb is used since the transition energy of Rb.III is almost exactly the same as the transition energy $5^2P_{1/2} \quad F = 3 \rightarrow 5^2P$ in ^{85}Rb .

²A more comprehensive analysis of the $5S$ & $5P$ energy levels of ^{87}Rb can be found in the Appendix C.

In the end, from the bulb lamp, the reference cell of the system will receive only photons associated with the Rb.II transition.

Electrons Excitation and Interrogation Having explained the excitation source, we can now proceed understanding how this energy is used over the atoms present in the *reference cell* (see Figure 4, also referred to as *vapor gas cell*) and in particular what's the cycle that electrons are forced to.

For the simplicity of explanation, we will consider the different stages of the electrons as if they happen in a temporal sequence. However, it's important to remind that these stages are not sequential but they happen simultaneously.

We can define three different stages in the cycle of the electrons:

- Optical pumping (population inversion and decay): the laser source coming from the bulb lamp excites the atoms to a higher energy level and a population inversion is created between the two hyperfine states $5S_{1/2}F = 1$ and $5S_{1/2}F = 2$.
- Microwave excitation: the microwave signal coming from the local oscillator excites the atoms and, if it's in resonance with the Rb.I transition, it force the population accumulated in the $5S_{1/2}F = 2$ state to fall back to the $5S_{1/2}F = 1$ state.
- Optical pumping (interrogation): the same laser used for population inversion is now used to interrogate the atoms and understand if the microwave signal was in resonance with Rb.I transition or not.

To better understand the cycle of the electrons, we can refer to Figure 8.

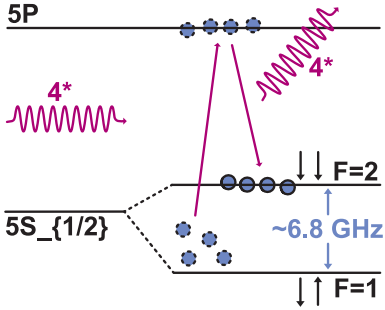


Figure 5: Population inversion and decay.

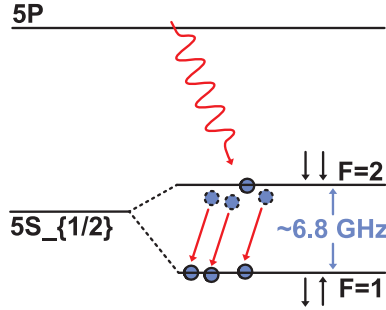


Figure 6: Microwave excitation.

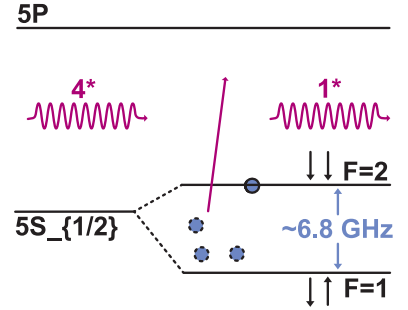


Figure 7: Optical interrogation.

Figure 8: Electrons cycle in a MODR-based CSAC due to the optical pumping, microwave excitation, and optical interrogation.

With reference to Figure 8, we can now analyze deeper the different stages of the cycle and understand how it's possible to detect whether the microwave signal is in resonance with the atomic transition or not.

In particular, in Figure 5 we can see four high energy photons coming from the pumping source that excite the electrons found at $5S_{1/2}F = 1$, to $5^2P_{1/2}$ state. From here, electrons will decay to both the $5^2S_{1/2}F = 2$ and the $5^2S_{1/2}F = 1$ states. Over time however, the population will tend to accumulate on the $5^2P_{1/2}F = 2$ state given that the excitation photons are not coupled with the Rb.III transition (due to the filter cell action).

During the second stage (Figure 6 for reference), the microwave excitation coming from the local oscillator is used to force the decay of the electrons from the $5^2S_{1/2}F = 2$ state to the

$5^2S_{1/2}F = 1$ state. Notice, however, that the decay is possible only if the microwave signal is at the right frequency of the transition, that is Rb.I. In case the microwave signal is not exactly in resonance with the atomic transition, not all the electrons will be forced to decay and some of them will remain in the excited state. Figure 6 shows an example where the microwave signal is not in perfect resonance with the atomic transition and 1 out of the 4 electrons remain in the $5^2S_{1/2}F = 2$ state.

Finally, the cycle is closed with the interrogation phase (Figure 7). Here, by sending the same amount of irradiation as in the pumping phase, we are able to detect if electrons are in the $5^2S_{1/2}F = 1$ state or in the $5^2S_{1/2}F = 2$ state. In particular, in case not the entire population has decayed to the $5^2S_{1/2}F = 1$ state during the microwave excitation, the interrogation phase will show a different intensity of the transmitted light. In Figure 7, we can see that 1 out of the 4 photons will be transmitted given that only 3 atoms are in the $5^2S_{1/2}F = 1$ state.

By measuring the intensity of the transmitted light, we can understand if the microwave signal was in resonance with the atomic transition or not.

Photodetector At the end of the vapor gas cell, a photodetector is used to measure the intensity of light transmitted through the reference cell.

In case of a MODR-based CSAC, only if the microwave signal was in resonance with the atomic transition, most of the laser source from the bulb lamp will be absorbed by the atoms and the transmitted light will be minimal. Conversely, in case of a non-resonant microwave signal, the intensity of the transmitted light will be stronger.

The signal captured by the photodetector is then sent to the control loop that will use it to fine-tune the local oscillator frequency.

3.2.2 Coherent Population Trapping (CPT)

In case of a Coherent Population Trapping (CPT) based system, the PP contains a vapor gas cell that receive a high energy signal from a laser source and force the valence electron of the Cesium (Cs) atoms to a coherent superposition of the two hyperfine ground states. If this coherent superposition happens, the electron is said to be *trapped in a dark state*, given that the incoming laser source will no more be coupled with the electron transitions and the atoms will not absorb the photons.

Similarly to the MODR, by measuring the intensity of the transmitted light, we can understand if the local oscillator was in resonance with the atomic transition or not.

In order to better visualize the operation of a CPT-based CSAC, we leave here a schematic representation of its PP (Figure 9).

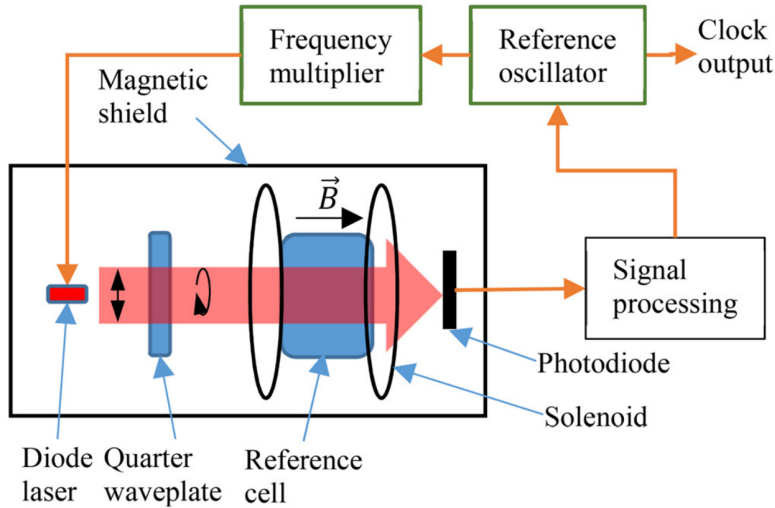


Figure 9: CPT-based CSAC scheme. Source [19].

Target Electron Transitions of Cesium (Cs) In case of PP based on CPT, the vapor gas cell is typically filled with Cesium (Cs) (^{133}Cs) atoms. Cs is an alkaline metal with a relatively simple electronic structure, defined as $[Xe]6s^1$. Its first ionization energy is 3.894eV , and the valence electron can be exited using relatively low energy photons. For these reasons, Cs is widely used in atomic clocks, as it allows for precise manipulation of the valence electron while containing the energy required for the excitation.

In particular, by recalling the quantum energy levels of ^{133}Cs (defined by quantum effects and interactions between the electron and the nucleus), we can better define our working frame for the CPT architecture. Three different transitions are of interest regarding the ^{133}Cs atom³:

$$\text{Cs.I } 6^2S_{1/2} \quad F = 3 \rightarrow 6^2S_{1/2} \quad F = 4: \approx 9.2\text{GHz}$$

$$\text{Cs.II } 6^2S_{1/2} \quad F = 3 \rightarrow 6^2P_{1/2}: \approx 895^{-}\text{nm}$$

$$\text{Cs.III } 6^2S_{1/2} \quad F = 4 \rightarrow 6^2P_{1/2}: \approx 895^{+}\text{nm}$$

Notice that the transition $6^2S_{1/2} \rightarrow 6^2P_{1/2}$, of $\approx 895\text{nm}$, is usually referred to as *D1 line*.

Quantum Superposition Before moving on and understanding the different components of the CPT-based CSAC, it's important to understand the concept of quantum superposition as it will be the key in the operation of the system.

In quantum mechanics, a quantum superposition is a fundamental principle that states that linear combinations of solutions to the Schrödinger equation are also solutions of the equation itself. In other words, if $|\psi_1\rangle$ and $|\psi_2\rangle$ are solutions of the Schrödinger equation, then $\alpha|\psi_1\rangle + \beta|\psi_2\rangle$ is also a valid solution of the state of the system. A valid quantum superposition can be generally defined as:

$$|\psi\rangle = c_\alpha |\psi_\alpha\rangle + c_\beta |\psi_\beta\rangle \quad (4)$$

Where $|\psi_\alpha\rangle$ and $|\psi_\beta\rangle$ are two different energy configurations of the system and c_α and c_β are complex numbers. Practically speaking, this means that the electron can be found not only in $|\psi_\alpha\rangle$ or $|\psi_\beta\rangle$, but also in any a superposition of the two states (with a probability defined by the complex numbers).

To facilitate the understanding of this counterintuitive concept, we report two different interpretations of the quantum superposition:

³A more comprehensive analysis of the $6S$ & $6P$ energy levels of ^{133}Cs can be found in the Appendix D.

- Bloch Sphere representation: by imagining the electron as a 3D sphere with a finite radius, we can imagine to represent its energy level (i.e. its state) using a spatial vector with the origin in the center of the sphere and the tip on the surface. By mapping the ground state with an upward vector (Figure 10) and the excited state with a downward vector (Figure 12), we can intuitively understand that any other direction the vector might assume, must be associated with a valid state of the electron (i.e. a valid quantum superposition).
- Modal interpretation: given that to each energy level of the electron is associated a wave function, we can interpret the quantum superposition as a linear combination of the wave functions associated with the different energy levels. This interpretation derives from the approach used in classical vibrations problem, where the superposition of different modes (i.e. waves of different frequencies) can be used to describe the vibration of the system. In figure 14, we can see the superposition of two different modes that generate a new wave function.

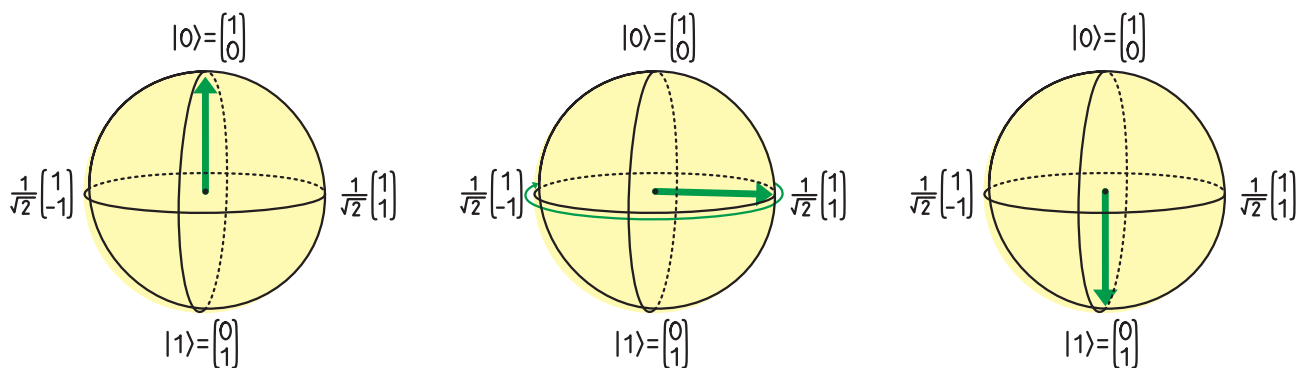


Figure 10: Ground state.

Figure 11: Superposition state.

Figure 12: Excited state.

Figure 13: State superposition via Bloch sphere representation.

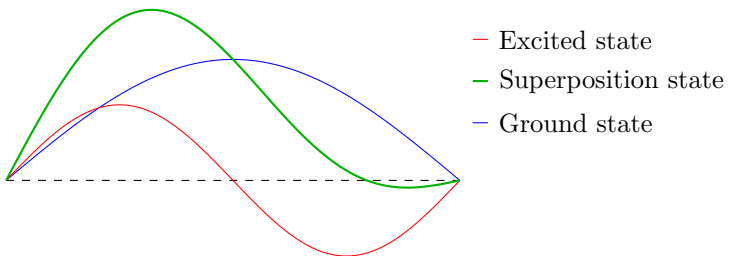


Figure 14: State superposition via modal interpretation and wave functions.

Λ-Lambda System & Dark State We can proceed and understand how the states' superposition is used related to the operation of a CPT-based CSAC. To do so, we need to introduce the concepts of Λ-Lambda system and dark state.

A Λ-Lambda system is a quantum system composed of three energy levels (see Figure 15 for reference), where not all the dipole transitions are allowed. In particular:

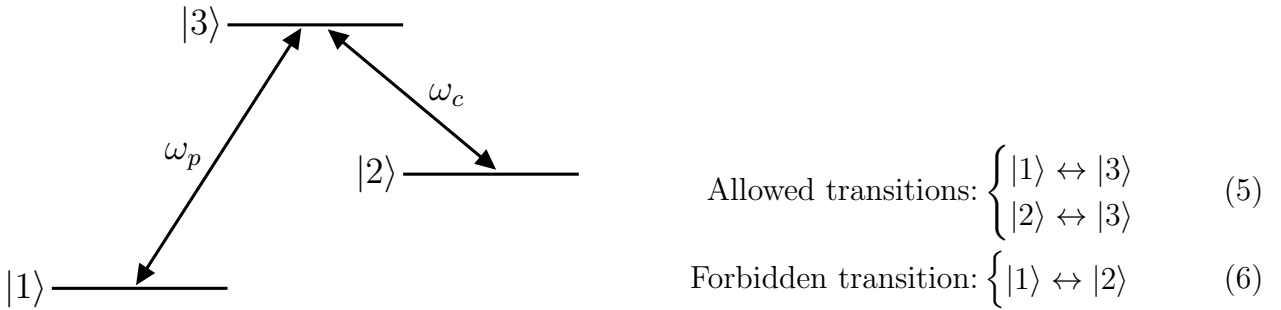


Figure 15: Λ -system representation. Source [25].

In case the system is excited with a stable and well-controlled laser source (more comprehensive explanation given in the following paragraph) that couples at the same time both $|1\rangle \leftrightarrow |3\rangle$ and $|2\rangle \leftrightarrow |3\rangle$ transitions, electrons will be pumped at first in their excited state (i.e. $|3\rangle$) and then forced to decay to $|\psi\rangle$, a superposition of $|1\rangle$ and $|2\rangle$. This method is called *coherent population trapping* and the system is said to be in a *dark state* given that the incoming laser source will no more be coupled with the electron transitions and the atoms will not absorb the photons. In our working frame, the Λ -system is composed of the two ground states $6^2S_{1/2}F = 3$ & $6^2S_{1/2}F = 4$ and the excited state $6^2P_{1/2}$ of the ^{133}Cs atom.

Pumping Source From now on, given for granted the concept of quantum superposition and Λ -system, we can step into understanding the components used to excite the ^{133}Cs atoms and obtain the desired dark state.

In a CPT-based CSAC, the pumping source is typically a *diode laser* (see Figure 9 for reference), and most commonly a *Vertical Cavity Surface Emitting Laser (VCSEL)*. The use of a diode laser instead of a bulb lamp is due to the need of a stable and well-controlled source of irradiation that can be precisely modulated based on the local oscillator frequency. In fact, VCSEL is a semiconductor laser diode that emits light from its top surface and it's characterized by a very narrow emission spectrum and a high modulation bandwidth.

In the framework of CSAC, the diode laser is driven by the local oscillator frequency and it's modulated in both Amplitude (AM) and Frequency (FM). In particular, in order to obtain the desired effect of coherent population trapping inside the reference cell, the laser source must meet the following requirements:

- AM modulation: the signal generated via the AM modulation must be at half the Cs.I frequency (i.e. half the transition frequency of the ^{133}Cs ground states hyperfine splitting);
- FM modulation: the signal generated via the FM modulation must be at frequency of the *D1 line* (i.e. the transition frequency of the ^{133}Cs ground state to the ^{133}Cs excited state).
- Circular polarization: the laser source must be positively circularly polarized.

The first two requirements can be easily met by controlling the injection current of the diode laser in time and are equivalent to state that the laser source must be the sum of a signal modulated at Cs.II with another modulated at Cs.III frequency. In other words, the laser source must be able to generate the beating wave of the two frequencies as shown in Figure 16. The third requirement can be met by using a quarter-wave plate in front of the laser source that convert the linear polarization of the source in a circular one (again, see Figure 9 for reference).

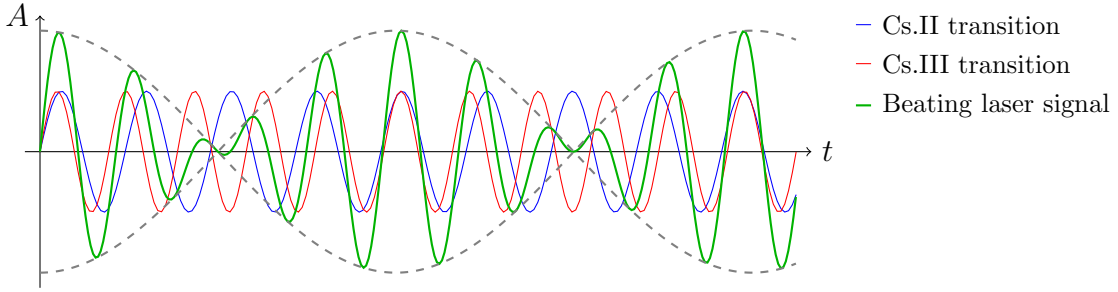


Figure 16: Beating wave of the laser source in a CPT-based CSAC (AM modulation is highlighted with a dashed gray line, FM modulation is clearly visible on the green wave).

Notice, however, that the one represented in Figure 16 is the ideal case where the laser source is perfectly modulated at the two frequencies Cs.II and Cs.III. In reality, the laser source is driven by the local oscillator frequency and some modulation errors will appear. Those shift with respect to the ideal case will give us the information needed to understand if the local oscillator is in resonance with the atomic transition or not.

Electrons Excitation and Interrogation Having explained the requirements of the excitation source, we can now proceed understanding how this energy is used over the atoms present in the *reference cell* (see Figure 9, also refereed to as *vapor gas cell*) and in particular what's the cycle that electrons are forced to.

For the simplicity of the explanation, we will consider the different stages of the electrons as if they happen in a temporal sequence. However, it's important to remind those stages are not sequential but they happen simultaneously.

We can define three different stages in the cycle of the electrons:

- Optical pumping (population inversion): the laser source coming from the diode laser excites the atoms from both the $6S_{1/2}F = 3$ and the $6S_{1/2}F = 4$ ground hyperfine states to the $6^2P_{1/2}$ excited state.
- Decay to the dark state (superposition state): if the laser source during the pumping stage was modulated properly as described in the previous paragraph, then the excited electrons will now decay to a coherent superposition of the two ground states $6S_{1/2}F = 3$ and $6S_{1/2}F = 4$. The atoms are now in a dark state.
- Optical pumping (interrogation): the same laser used for population inversion is now used to interrogate the atoms and understand if the local oscillator frequency was in resonance with the atomic transition Cs.I or not.

To visualize the cycle of the electrons, we can refer to Figure 20.

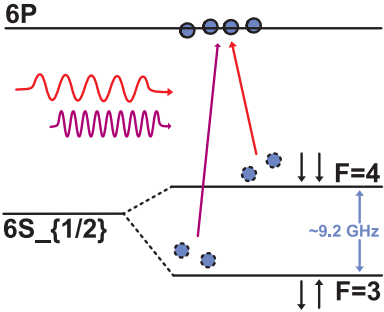


Figure 17: Population inversion.

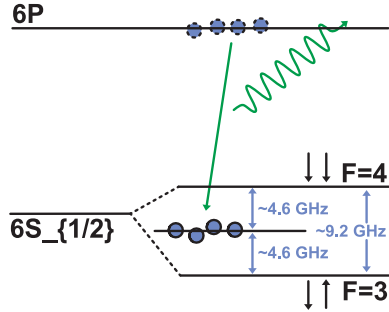


Figure 18: Population decay.

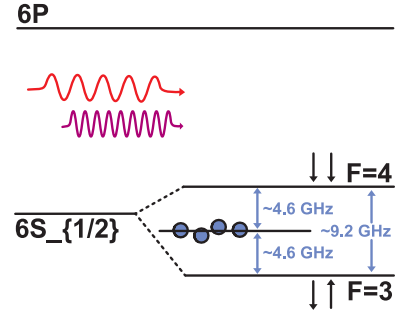


Figure 19: Optical interrogation.

Figure 20: Electrons cycle in a CPT-based CSAC due to the optical pumping, decay and optical interrogation.

For the sake of the explanation and simplification, we will consider the pumping laser source (the one coming from the diode laser) as two separate signals, one modulated at the frequency Cs.II and the other modulated at Cs.III, even if in reality a single beating wave of the two frequencies is used (Figure 16).

In Figure 17, we can see four electrons that get excited from $6S_{1/2}F = 3$ and $6S_{1/2}F = 4$ ground hyperfine states to the $6^2P_{1/2}$ excited state.

Being $6^2P_{1/2}$ an unstable state, electrons will start to decay to the non-excited states. In Figure 18, we can see that over time the population will tend to accumulate in a coherent superposition of the two ground states, given that from here the electrons won't be coupled to the laser source anymore. Notice, however, that the accumulation in the superposition state is possible only if the laser source was properly modulated, that is equivalent to say that the local oscillator was in resonance with the atomic transition Cs.I.

Finally, the cycle is closed with the interrogation phase (Figure 19). Here, by sending the same amount of irradiation as in the pumping phase, we are able to detect if electrons are in the superposition state or not. In Figure 19, we can see that all the electrons are found in the superposition state and so the intensity of the transmitted light will be maximal since none of those electrons is coupled with the laser source.

By measuring the intensity of the transmitted light, we can understand if the local oscillator was in resonance with the atomic transition or not.

Photodetector At the end of the reference cell, a photodetector is used to measure the intensity of the transmitted light.

In case of a CPT-based CSAC, given that if the microwave signal was in resonance with the atomic transition, most of the electrons are now in the dark state, then the intensity of the transmitted light will be maximal. Conversely, in case of a non-resonant microwave signal, the intensity of the transmitted light will be lower (a fraction of the light will be absorbed by electrons that are not in the dark state). In Figure 21, we can see an example of a detuned signal captured by the photodetector.

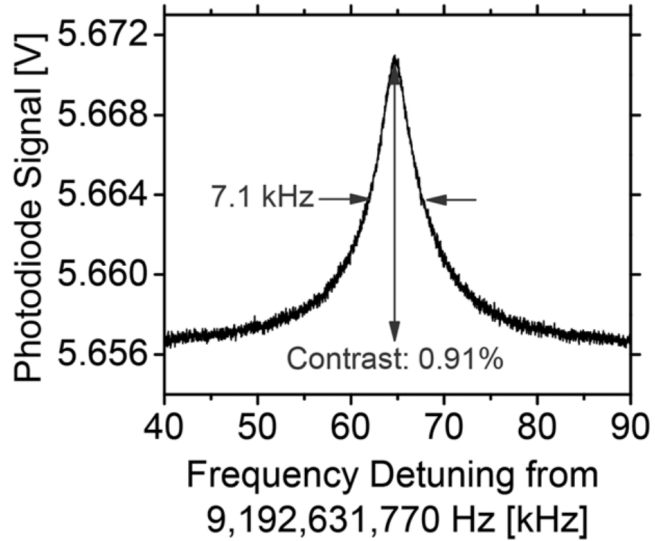


Figure 21: Detuned photodetection signal in a CPT-based CSAC. Source [19].

The signal captured by the photodetector is then sent to the control loop that will use it to fine-tune the local oscillator frequency.

3.3 Control Loop (CL)

The Control Loop (CL) act as the brain of the clock, adjusting dynamically various parameters inside the CSAC architecture to optimize stability and output frequency accuracy. To do so, multiple servo loops based on PI⁴ controllers are implemented to control specific areas and properties of different components. CL takes as input the signal coming from the Physics Package (PP) and other sampled quantities coming from a network of sensors that are used to monitor the state of the clock (e.g., temperature sensors, magnetic field sensors, etc.)

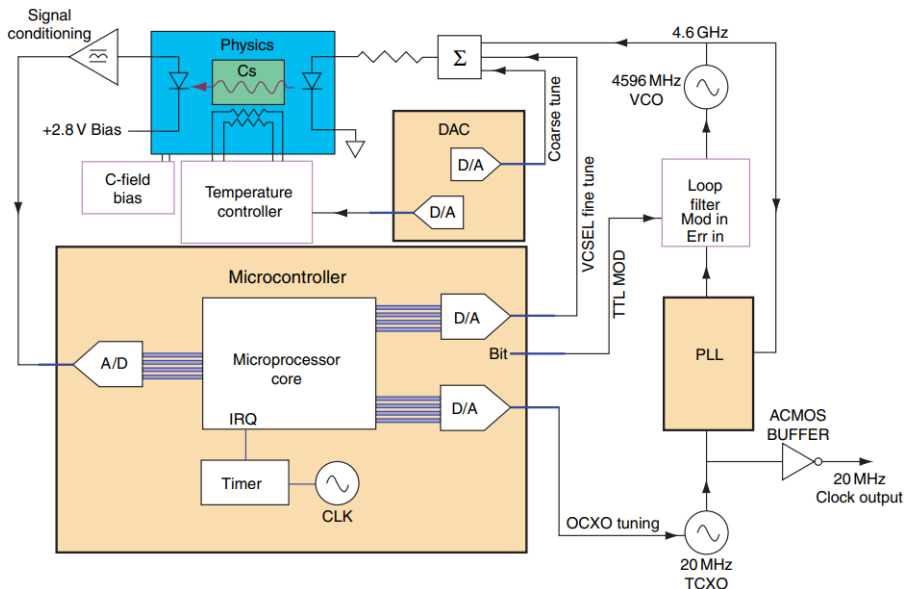


Figure 22: Control Loops block diagram for a CPT-based architecture (note the presence of the VCSEL). Source [20].

In Figure 22 some key components are highlighted, such as microcontroller, converters (DAC and ADC), and PLL (Phase-Locked Loop) that are crucial for the correct functioning of the

⁴Proportional Integral

CL. In particular, the PLL is responsible for keeping in phase the LO (indicated by the label "TCXO" in the bottom right) with the FS, minimizing the phase noise and the frequency drift between the two components.

In a regular architecture, at least four servo loops are implemented to target different parameters.

Local Oscillator frequency servo loops The most important task of the CL is the discipline of the Local Oscillator (LO) frequency to the desired value, locking it to the atomic resonance frequency or one of its multiple harmonics.

To achieve this, the CL receives the output signal from the PP and generate a feedback voltage signal that is sent to the LO group. Here, it's converted in a temperature variation of the crystal in order to modify its mechanical properties, thus adjusting the output frequency.

With reference to Figure 22, we can see this control line in the bottom right corner of the image, associated with the label "OCXO tuning", going from the microcontroller unit to the LO group.

It has to be noted that the LO has a much slower dynamics with respect to the electrical one provided by the microcontroller. This causes an unavoidable delay over the feedback loop action and the actual effect on the LO output frequency.

Laser frequency servo loops In case of the use of VCSEL as the excitation source, the CL is also responsible for the control and tuning of its frequency that can be affected by external factors such as temperature variations or electrical/magnetic disturbances.

The diode laser is controlled by the summation of three different signal (see Figure 22), that are the coarse tune, the fine tune, and the FS output.

In particular, the coarse tune signal is independent of any state of the clock and doesn't vary during the operation time. The fine tune instead, is generated by the microcontroller and is used to compensate the environmental effects that cause a drift in the frequency of the excitation source. Finally, the FS output is added in order to permit the PP to understand if the LO is locked to the atomic resonance frequency.

Laser and cell temperature servo loops Maintaining constant temperatures for the laser and the reference cell within the PP is another job of the CL.

As we will see in the next section (Section 4), the temperature of these two components are crucial for the performances of the clock and should be maintained at a constant value during the operation time.

To do so, the feedback loop modify the temperature based on the signal coming from a network of thermocouple sensors that are placed near the targets. Notice how, depending on the specific architecture of the clock, the CL can act on the temperature of the two components independently or together.

In this way, the CL ensures that both the excitation source and the atomic resonance frequencies are not affected by temperature variations, improving the photons coupling effectiveness.

Other servo loops In addition, other control loops can be implemented to target other parameters that might affect the performances of the clock.

Among these, one of particular importance is the servo used to shield or more in general control the magnetic field surrounding the PP. Again, with reference to Figure 22, we can recognize this control line in the bottom left corner of the "Physics" package block, associated with the label "C-field bias".

This control loop is used to maintain a zero or a constant value of the magnetic field inside the PP, ensuring a precise and predictable behavior of the atomic resonance frequency that otherwise might suffer from frequency shifts (Zeeman and Stark effects, see Section 4).

3.4 Local Oscillator (LO)

The Local Oscillator (LO) is responsible for generating the effective output frequency of the clock.

Generally speaking, the LO is quartz crystal based component that generates a stable frequency near its resonance point by leveraging the mechanical vibrations of the crystal. However, begin a mechanical component, it's subject to temperature variations that can affect its output frequency. For this reason, an appropriate servo loops is implemented in order to keep it to a constant temperature and stabilize its output frequency (see Section 3.3).

Typically, the LO is kept running at $10MHz$ or $20MHz$ in order to have a high compatibility with the existing electronics devices. Its value is then compared with the atomic one by adopting a Frequency Synthesizer (FS) that multiplies its frequency by a fixed factor. As we have briefly explained in previous sections, to achieve this, a PLL is used to keep in phase the LO with the FS, minimizing the phase noise and delay that might occur between the two.

In the next section (Section 4), we will see that the performances of the entire clock are heavily dependent on the performances of the LO, in particular in the short-term stability. For this reason, the LO is one of the most critical components of the CSAC and should be carefully chosen based on the specific application of the clock.

LO Types and Considerations There exist many types of LO that can be used in a CSAC, each with its own characteristics and performances. The most commonly used are both the TCXO⁵ and the OCXO⁶, given their good intrinsic stability and the possibility to be precisely controlled by a temperature ambient variation. However, is important to note that the OCXO is generally more power-hungry, bulky, and expensive compared to the TCXO, making it unsuitable for applications having strict constraints on these parameters. On the other hand, OCXO are generally more stable and have a lower phase noise compared to TCXO, making them more suitable for high-performance applications.

As for many other components of the CSAC, the choice of the LO is strictly dependent on the specific application and constraints of the clock.

4 Performances and Limitations

Now that we have defined the core concept and individual components of a CSAC, we can proceed evaluating its performance and limitations using the metrics defined in Section 2.

In order to do so, we will consider and analyze the main disturbances effects that affect the overall performances, see what are the current solutions proposed and what they imply in terms of limitations and trade-offs.

⁵Temperature Controlled Crystal Oscillator

⁶Oven Controlled Crystal Oscillator

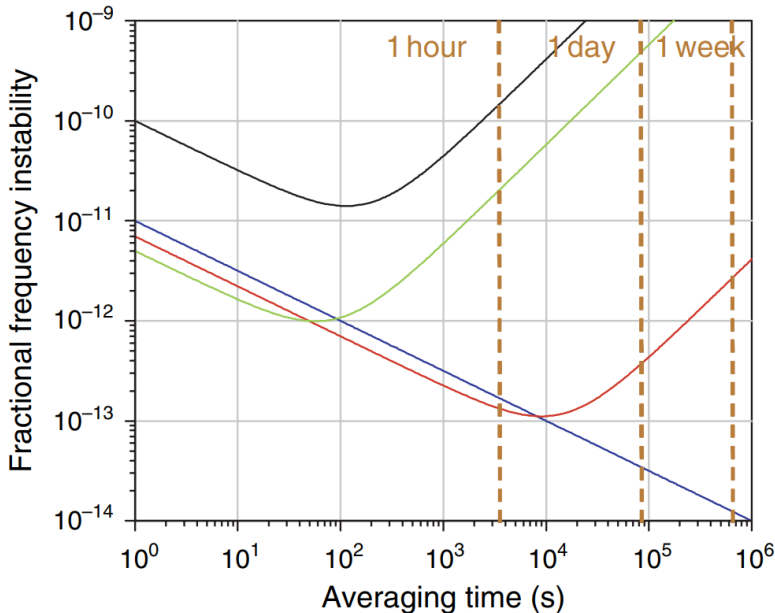


Figure 23: Allan deviation plot $\sigma_y(\tau)$ for different clock type sources (Cesium (Cs) Beam Standard, Rubidium (Rb) vapor cell clock, Oven-controlled crystal oscillator (OCXO), Temperature-compensated crystal oscillator (TCXO)). Source [20].

In Figure 23, it's visible a comparison of the Allan deviation $\sigma_y(\tau)$ for different clock sources. Medium to long-term stability is represented, ranging from an average τ scale of 10^0 to 10^6 seconds, and is clearly visible how atomic clocks (both the Rb vapor cell and the Cs beam standard) outperform crystal oscillators in terms of stability. However, it's important to notice that the Cs beam standard isn't a CSAC, but a traditional table-size atomic clock. And also the Rb vapor cell clock represented in the plot is a Miniature Atomic Clock (MAC), which is larger and more power-hungry than a CSAC. Typically, a CSAC is expected to have a stability $\sigma_y(\tau = 1s) \approx 10^{-11}$, and the flicked floor at around $\tau = 10^4$ s, positioning itself in between the TCXO and the OCXO in the short to medium-term stability range and outperforming them in the medium to long-term stability range.

4.1 Short-term frequency stability

Short-term stability is strictly related to the Fast Noise of the local oscillator.

It's usually referred to very small time scale, in the order of $\tau < 1s$, and most of the time is not of real importance for real-world applications, where the main focus is on the medium and long-term stability. However, in some particular cases, such as scientific experiments at the nanosecond scale, the short-term stability can be a key factor to consider.

Generally, we can expect to have a stability of $10^{-11} \leq \sigma_y(\tau = 1s) \leq 10^{-10}$.

The most straightforward way to mitigate the Fast Noise is to improve the quality of the local oscillator (i.e. going from a TCXO to an OCXO), but this implies an increase in the power consumption and the size of the clock, which is not always possible in portable applications. Another possibility would be to increase the frequency of the local oscillator, but then an appropriate frequency dividers would be required to obtain an output in the common electronic frequency range (10Mhz), increasing the overall size of the clock.

4.2 Medium-term frequency stability

Medium-term stability, instead, is one of the key metrics for all the applications where a CSAC is used.

It can be computed as stated in Equation 3 and is governed mostly by the stability of atomic interactions and energy levels. Many factors can affect this type of stability, such as temperature of the environment, magnetic field, and quality of the excitation source.

Generally, we can expect to have an increasing stability from $10^{-10} \text{ at } \tau = 1\text{s}$ to $10^{-12} \text{ at } \tau = 10^4\text{s}$. However, medium-term stability is strictly dependent on the quality of the physics package, its components and the design choices made to mitigate the disturbances. The main disturbances together with some possible solutions (that always imply trade-offs) are listed below.

Rubidium vs. Cesium As we have seen, both Rb and Cs can be used as the atomic element inside the reference cell of a CSAC.

However, it has to be noted that the splitting gap in the two hyperfine ground levels is not the same for the two elements. In fact, comparing Rb.I and Cs.I transitions, we can see that the frequency of the Rb transition is around 6.8GHz , while the Cs transition is around 9.2GHz . By recalling Equation 3 for the medium-term stability, we can observe that the stability is inversely proportional to the line quality factor Q . Being $Q = \frac{\nu_0}{\Delta\nu}$, we can understand that the higher the frequency of the transition, the higher the stability of the clock. So, in theory, a Cs-based clock should have a better stability than a Rb-based one.

On the other hand, the Rb has a simpler and easier to control pumping system that has a better coupling efficiency with the atomic resonance frequency with respect to the diode laser used in the Cs clock.

For this reason, the performance of the two clocks is quite similar, with the Cs clock being slightly better in terms of power consumption and size, but with a more complex and expensive physics package.

Gas pressure and composition inside the reference cell Collision with untreated interior walls of the reference cell can depolarize the spin of electrons, forcing them to return to the ground state. For this reason, the signal in output from the Physical Package will be reduced (*SNR* reduction) and also the medium-term stability will be affected.

To mitigate this effect, the reference cell is usually filled with a precise combination of gases, such as Helium, Neon, Argon or Nitrogen. Those gasses help in reducing the number of collisions of the Rubidium or Cesium atoms with the inner wall, enhancing the possibility of electrons to remain in the excited state for a longer time, increasing the signal-to-noise ratio *SNR*.

However, we know that the gas pressure inside the reference cell depends also on the temperature. For this reason, the temperature of the reference cell must be kept constant to ensure a stable gas pressure and composition. This is also done via a dedicated servo loop as explained in Section 3.3. However, the use of a dedicated thermo-stabilizing system implies an increase in both the power consumption and the size of the clock.

Quality of the excitation source Another key factor that can affect the stability of the CSAC is the quality of the excitation source.

Both the bulb lamp and the diode laser are dependent from the temperature. A small variation in frequency can reduce the coupling between the excitation source and the atomic resonance frequency, affecting the medium-term stability of the clock. For this reason, the temperature of the laser source must be tuned accordingly by an appropriate servo loop.

If we consider a VCSEL source (as in the case of a CPT-based clock), the temperature sensibility is around 300GHz/K , which means that even a very small temperature variation can greatly shift the frequency of the laser source, reducing the number of electrons in the dark state, thus decreasing the signal-to-noise ratio *SNR*.

Magnetic field (Zeeman effect) The presence of an external magnetic field can also significantly affect the accuracy of the CSAC.

The Zeeman effect is a phenomenon that splits the atomic energy levels into multiple sublevels when an external magnetic field is applied. By doing so, the atomic resonance frequency is shifted, affecting the accuracy of the clock. In particular, the magnitude of the Zeeman shift is proportional to the strength of the magnetic field applied.

To mitigate this effect, the entire physics package is usually shielded with a magnetic shield to reduce the impact of the external magnetic field on the atomic transitions. In some cases, the CSAC can also have an internal magnetic field, called *C-field*, to counteract the external one. If that is the case, an appropriate control loop is adopted to minimize the disturbance effect. Moreover, by applying a known magnetic field to the physics package, the Zeeman shift can be measured and used to precisely calibrate the clock.

Optical instabilities (Stark effect) Similarly to the Zeeman effect, the Stark effect can also shift the atomic energy levels, affecting the accuracy of the clock.

The Stark effect is a phenomenon that occurs when an oscillatory external electric field interacts with the charged nucleus and electrons within the atom, modifying their energy. In case of a CSAC, the excitation photon might be subjected to instabilities in intensity and/or spectral profile, inducing unintended Stark shifts that can cause deviations in the atomic resonance frequencies, leading to clock frequency instability.

Frequency shifts (Doppler effect) Finally, a huge source of disturbance for the CSAC is the Doppler effect.

Inside the reference cell in fact, atoms are continuously moving with random directions. In this way, even if the excitation frequency is carefully selected, a red or blue shift can occur depending on the atom velocity and the coupling between the source and the atomic resonance frequency can be reduced. This implies a reduction in the signal-to-noise ratio and a decrease in the medium-term stability of the clock.

A proposed solution is to reduce the mean-free-path of the atoms, by reducing either the pressure or the temperature inside the reference cell. However, in order to achieve this, more thermal power stabilization is required.

4.3 Long-term frequency stability

Long-term stability refers to the ability of maintaining frequency accuracy over extended periods (hours, days or even months).

Here, all the previously mentioned disturbances can have a significant impact. The aging of the components is also relevant and to be considered. Over longer periods of time, the pressure inside the reference cell might change, the quality of the excitation source might degrade, and so also the mechanical properties of the local oscillator.

Temperature exposition is also a key factor in the long-term stability of the clock. If excessive temperature is applied for long periods of time, the gas pressure inside the reference cell will increase and also the vacuum integrity of the entire clock would be affected. Moreover, the electronics circuits degrade faster at higher temperatures, reducing the overall lifetime of the clock.

4.4 Frequency Stability vs. Size, Weight, and Power (SWaP)

As we have seen in the previous paragraphs, a strong correlation exists between the stability of the clock and its size, weight, and power consumption. To achieve better performances, a

series of internal components must be increased in size (e.g. the reference cell) or quality (e.g. the local oscillator), or additional servo loops must be added to control the disturbances (and indeed more sensor and actuator are required).

So qualitatively, we can understand how better performances are associated with an increase in the SWaP of the clock. In Figure 24, we can observe how the Allan deviation $\sigma_y(\tau = 1s)$ is related to the SWaP of the clock for different types of atomic clocks, ranging from the traditional table-size atomic clock to the CSAC.

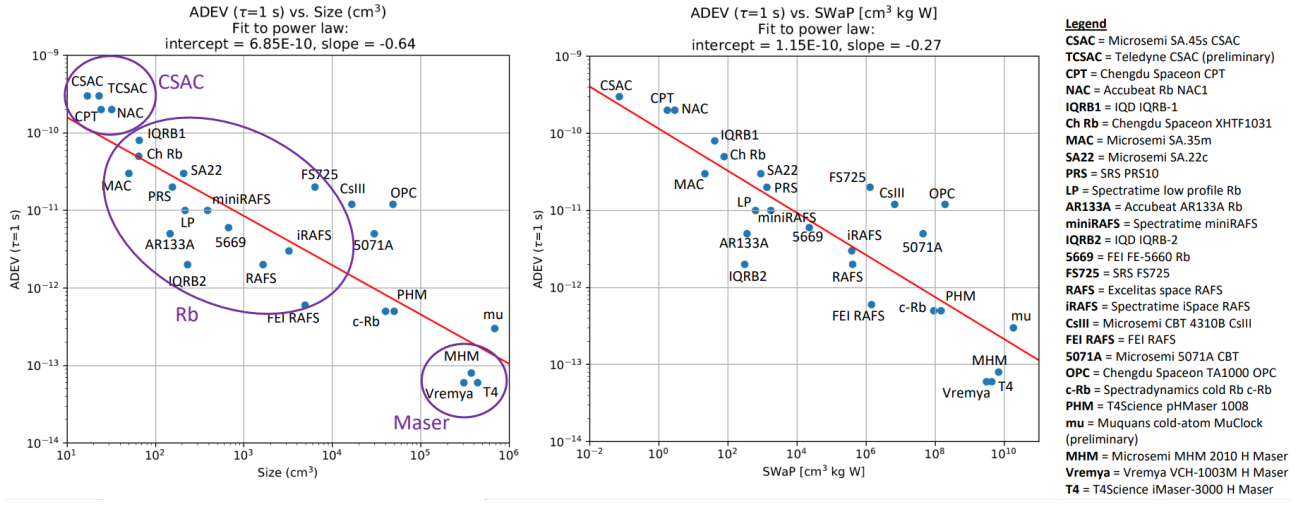


Figure 24: Allan deviation $\sigma_y(\tau = 1s)$ vs. Size, Weight, and Power (SWaP) for different atomic clocks. Source [11].

As also marked by the red lines in both the plots, it's clear that a correlation exist and that is not possible to achieve a very high stability without a significant increase in the SWaP of the clock. In particular, the equations of the two red lines are⁷:

$$\sigma_y(\tau = 1s) = 6.85 \times 10^{-10} + \text{volume}^{-0.64} \quad (7)$$

$$\sigma_y(\tau = 1s) = 1.15 \times 10^{-10} + \text{SWaP}^{-0.27} \quad (8)$$

5 Applications

As we have seen in Section 4, the performance of a CSAC varies depending on multiple factors that modify the nominal behavior of the internal components and the overall functionality of the clock.

However, the possibility of choosing components with different characteristics and the flexibility of the design, allows CSAC to be used in a wide range of applications. In the following, we will give an overview of the main applications that relies on CSAC technology highlighting the requirements and the role the clock has in the application. Here, applications are listed in order of their impact on society, starting from the most commonly used to the most specialized ones.

5.1 Global Navigation Satellite System (GNSS)

The Global Navigation Satellite System (GNSS) is a satellite-based system that delivers geolocation and time information to any GNSS receiver that is able to receive contemporaneously

⁷The units adopted in the equations related to the SWaP are: Size and Volume [cm^3], Weight [kg], Power [W]

signals from multiple satellites. The GNSS system is adopted in a wide range of networks and applications, including the Global Positioning System (GPS), Galileo⁸, GLONASS⁹, and it is used in military, scientific, and commercial applications. Basically, every application that requires a precise time reference and/or a precise position retrieve the information from the GNSS system.

The process used to calculate the position of the receiver is based on the *trilateration* method, which compute the distance between the receiver and the satellites by measuring the time of the light signal to travel from the sender to the receiver. Theoretically, the position of the receiver can be calculated by using the signals from three satellites, but in practice, a fourth satellite is used to correct the time offset of the receiver's clock. In fact, under a mathematical point of view, the system to be solved is composed of four equations and four unknowns, where the unknowns are the position of the receiver in space and the time offset of the receiver's clock.

$$\Delta d_i = c \cdot (\Delta t_i + \delta t) = \sqrt{(x_r - x_i)^2 + (y_r - y_i)^2 + (z_r - z_i)^2}, \quad i = 1, 2, 3, 4 \quad (9)$$

$$\underbrace{x_r, y_r, z_r, \delta t}_{\text{4 Unknowns requires 4 satellites}} \quad (10)$$

Role of CSAC Nowadays, the GNSS receiver usually uses a quartz crystal oscillator to generate the clock signal. However, this type of oscillator has a high drift rate, which means that the time offset of the receiver's clock can change significantly over time. This is also the reason why the fourth satellite is required to correct the time offset of the receiver's clock.

The CSAC technology can be integrated into GNSS receivers to provide a more accurate and in particular more stable time reference, which can avoid the need for the fourth satellite after the first calibration of the receiver's clock. This, in turn, open the possibility to have a precise position even in remote areas where the signal from the fourth satellite might not be available. Moreover, the inner stability allows for even a more precise trilateration, both in terms of latitude and longitude, and also in terms of altitude, which is usually the most difficult parameter to measure because of geometrical considerations.

5.2 Military Applications

Military applications of CSAC technology are many, ranging from secure communication systems to missile guidance systems.

A couple of examples are IED Jammers and SAASM.

IED Jammers IED (Improvised Explosive Device) jammers are devices that shield an area around the device from radio signals, preventing the detonation of IEDs by blocking the radio signals used to trigger them. To work properly, the frequency of this device must be precisely adjusted, and no drift are permitted. Moreover, since a single jammer has a limited range, multiple jammers are often employed to cover a larger area. If this is the case, the networks require each node to work in a perfectly synchronized way, given that a small shift in frequency can lead to a possible failure in the entire network.

In order to accomplish this, each IED jammer device usually integrate a CSAC. Its capabilities of better holdover with respect to other oscillators, allows longer time of operation without the need of recalibration.

⁸The European alternative to the American GPS

⁹The Russian alternative to the American GPS

SAASM SAASM (Selective Availability Anti-Spoofing Module) is a highly secure GPS module that provides decryption and encryption capabilities for GPS receivers. The module is in fact capable of sending and receiving longer GPS codes (encrypted P(Y) code) that are more resistant to jamming and spoofing attempts. To do so, the internal clock of the device must be capable of generating a signal with a very high stability and precision to avoid any possible error in the communication.

Traditionally employed quartz oscillator are not able to provide the required stability, leading to errors and securities issues in the communication. Instead, the stability over time of a CSAC meet the requirements of the SAASM module, allowing it to work properly and securely.

5.3 Ocean Bottom Seismics (OBS)

Another application that benefits from the CSAC technology is the exploration of the Earth's crust and mantle done via Ocean Bottom Seismics (OBS) technique. This technique consists of deploying a network of geophones on the ocean floor to measure the travel times of reflected or refracted seismic waves generated by earthquakes or artificially generated by air guns or explosives. The data collected by the geophones are then used to create a 3D map of the Earth's crust and mantle.

The oil exploration industry is one of the main user of this technique, as it helps estimate the location and depth of various features of interest, such as oil reservoirs and gas deposits.

Role of CSAC In order to work properly, the timestamp of each geophones must be accurate and coordinated with the others in the networks. However, the signal from the GNSS system is not available on the ocean floor, and the traditional quartz oscillator might not be able to provide the required stability over time.

CSAC instead, can be synchronized with the GNSS system before the deployment, and then work autonomously for weeks or even months on the ocean floor, providing a precise timestamp for the geophones. This method allows for a more accurate seismic mapping than the traditional one, where geophones are placed some meters below the surface ocean allowing them to communicate with the GNSS system.

5.4 Other Applications

Other fields that benefit from the CSAC technology are telecommunications and space experiments industries.

In particular, the telecommunications industry relies on precise time information to synchronize the network and ensure high speed communication. However, in case the GNSS signal became not available or the master clock fails, the network must be able to work autonomously for a certain amount of time. In this case, CSACs can be used to provide up to a local area a temporary time reference until the master clock is restored.

Another field where CSAC technology is employed are space experiments. Some example of successfully deployed CSACs in space are the SPATIUM (Space Precision Atomic-clock Timing Utility Mission) and the SPHERES (Synchronized Position Hold, Engage, Reorient, Experimental Satellites) projects. Both of them involved the use of CSACs to synchronize the satellites and/or to provide a precise time reference for the experiments while keeping size, weight, and power consumption low.

6 Future prospects

So far, we have analyzed the commercial available CSAC and observed how with the current architecture there exist a limitation in terms of achievable stability vs. size, weight and power consumption.

In this section, we will discuss the future prospects of CSAC technology, focusing on the motivations for the development of next-generation CSACs and the proposed solutions to overcome the current limitations.

6.1 Motivations for Next Generation CSACs

While current CSAC technology offers significant advantages in terms of miniaturization with respect traditional atomic clocks, there is still room for improvement under every aspect of the clock (stability, accuracy, SWaP, etc.).

As it has been with the development of the first CSAC, DARPA is again the main driver for the development of next-generation CSACs. Among the funded projects and collaborations with multiple research institutions, three main programs are worth mentioning:

- IMPACT: aimed to develop a CSAC with a volume of 20cm^3 , a power consumption of 250mW and a long-term stability of $\sigma_y(\tau = 1\text{month}) < 160\text{ns}$.
- ACES: aimed to develop a palm-sized, battery-powered CSAC with a $1000\times$ performance improvement with respect to the current commercial available CSAC.
- ROCkN: continuation of the ACES program, with the aim of further improving the performances of the CSAC.

The stability targets aimed by these DARPA programs are illustrated in Figure 25.

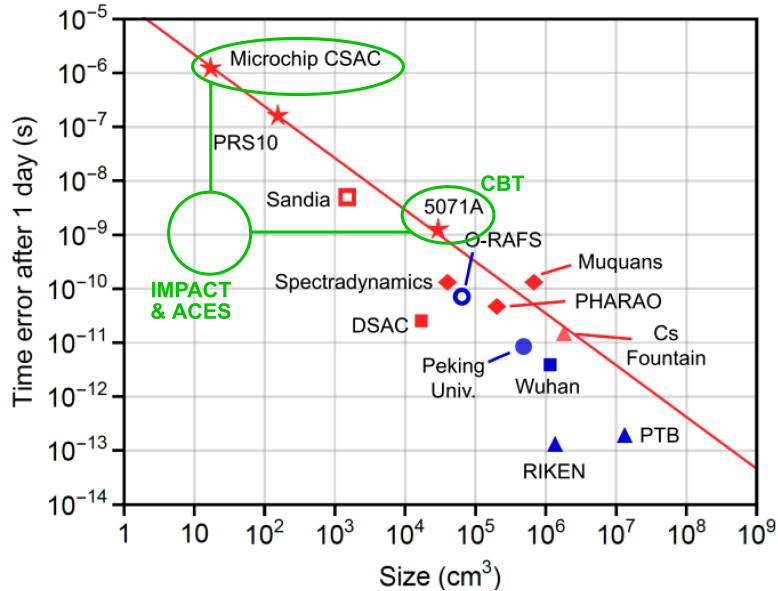


Figure 25: Stability targets for the DARPA IMPACT and ACES programs. Source [23].

Generally speaking, the next generation of CSACs aims to achieve similar quality in terms pf performances to the current Cesium Beam Tube (CBT) clocks, which are the current gold standard for high-precision timekeeping, while maintaining the advantages of the CSAC technology in terms of size, weight and power consumption.

6.2 Proposed research directions

To overcome the current limitations and deviate from the relation between stability and SWaP explained in Section 4.4, a different physics approach must be exploited.

After more than 15 years of development, three main research directions have been identified as the most promising for the development of the next generation of CSACs:

- Microwave transitions in laser-cooled alkali metals.
- Microwave transitions in double-resonance trapped ions.
- Optical transitions in warm atomic/molecular vapors.

In the following subsections, we will analyze the current state of the art of these research directions and the issues and challenges that need to be addressed to make them suitable for commercial applications.

6.2.1 Microwave transitions in laser-cooled alkali metals

The first research direction is based on the use of microwave transitions in laser-cooled alkali metals.

The use of cold atoms in the reference cell instead of warm atoms allows for a significant reduction in the Doppler broadening of the atomic transitions and the collisional shifts, which can be considered the main sources of frequency instability in the current CSAC technology. In the proposed architecture, both Rb and Cs atoms are laser-cooled and trapped in a 2D-MOT¹⁰, before being transferred to a dedicated interrogation cell. Here two distinct CPT light fields are used at first to prepare the atoms in a coherent superposition of states, and then to probe the atomic transitions based on the local oscillator frequency.

From a stability point of view, the results look promising as the Doppler broadening is significantly reduced and the line quality factor is greatly improved. The main bottlenecks however exist and are given by the technological and experimental limitations. In particular, pressure drifts of the atom source, imperfections in the CPT optical implementation, and technical noise on the lasers are the main sources of instability, rather than fundamental physics.

6.2.2 Microwave transitions in double-resonance trapped ions

The second research direction is based on the use of microwave transitions in double-resonance trapped ions. Up to today, this seems to be the most promising path as it allows for a significant reduction in the Doppler broadening and the possibility of miniaturization.

The working principle is very similar to the one of the laser-cooled alkali metals, but with the use of ions instead of atoms and a different cooling mechanism. In particular, both Ytterbium-171+ (Yb+) and Mercury-199+ (Hg+) based clocks have been developed and tested, showing excellent stability thanks to the Paul's trap mechanism.

A couple of fully functional prototypes have been developed, such as the Yb+ clock developed by Sandia National Laboratories and NASA's Jet Propulsion Laboratory (JPL) in 2015, and the Hg+ clock developed by JPL in 2019. Both of them already met the stability requirements imposed by the DARPA programs, but still face some challenges related in particular to Stark effect.

The use of electric fields for ion manipulation can cause a shift in the ions' transition frequency. To mitigate this, pulsed laser interrogation techniques are required, which indeed complicate the system design and the miniaturization of the components.

¹⁰2D Magneto-Optical Trap

On the other hand, the simplicity of the trapping system and the high manipulability of the ions make this approach the most promising in the optics of the next generation of CSACs.

6.2.3 Optical transitions in warm atomic/molecular vapors

The third research direction is based on the use of optical transitions in warm atoms environments.

The switching from a microwave range in the target transition frequency to a much higher energy (optical) range allow an increase in both the line quality factor and the signal-to-noise ratio, allowing for a significant improvement in the clock stability.

However, this approach is the most challenging from a technological point of view as it requires the development of a series of miniaturized components, such as Kerr-micro-resonator frequency combs, waveguides, and microfabricated photomultiplier tubes. Those components are still in the experimental stage and require further development to be suitable for commercial applications.

At the moment, some earlier version prototypes have been developed, such as the NIST Chip-Scale Optical Atomic Clock in 2019 and the NIST-DRAPER Miniature Atomic Clock in 2020. As in the case of the laser-cooled alkali metals or the double-resonance trapped ions, also these clock already met the stability requirements imposed by the DARPA programs, but still face some challenges related to the miniaturization of the components.

7 Conclusion

Chip-Scale Atomic Clocks (CSACs) represent a significant advancement in the field of atomic clocks, offering a miniaturized and low-power alternative to traditional atomic clocks. Their enhanced stability and accuracy thanks to the use of atomic transitions as a discipline reference for the local oscillator make them ideal for a wide range of applications, where precise timekeeping and size, weight, and power constraints are critical.

However, the physics enabling the operation of CSACs also poses significant challenges in a further step towards better performance and miniaturization. Due to the intrinsic limitations, also the applications involving CSACs often relies of some external reference to correct the drift and the aging on the long term.

To overcome these limitations, the development of the next generation of CSACs is an active area of research. After more than 15 years since the launch of the first program to develop the NG-CSACs, several technological solutions have been proposed, but a clear winner has yet to emerge.

The potential of NG-CSACs is vast, extending far beyond precise timekeeping. In case of success, these devices have the potential to revolutionize fields like microfabrication, quantum computing, and even our understanding of fundamental physics phenomena. We believe that pursuing the development goals set for NG-CSACs represents an investment in the future, paving the way for groundbreaking advancements across various scientific and technological disciplines.

References

- [1] Kateryna Aheieva, Rahmi Rahmatullah, Ryotaro Ninagawa, Ibukun Oluwatobi Adebolu, Hirokazu Masui, Takashi Yamauchi, Sangkyun Kim, Mengu Cho, Chee Lap Chow, Man Siu Tse, and King Ho Holden Li. Cubesat mission for ionosphere mapping and weather forecasting using chip-scale atomic clock. In *2017 Progress in Electromagnetics Research Symposium - Fall (PIERS - FALL)*, pages 761–766, 2017.
- [2] Thejesh N. Bandi et al. Advanced space rubidium atomic frequency standard for satellite navigation. *GPS Solutions*, 26(2):54, Mar 2022.
- [3] Parameswar Banerjee and Demetrios Matsakis. *Frequency Stability*, pages 79–108. Springer Nature Switzerland, Cham, 2023.
- [4] BIMP. Si base unit: second (s). <https://www.bipm.org/en/si-base-units/second>.
- [5] Jiaqi Cui et al. Design and studies of an ultra high-performance physics package for vapor-cell rubidium atomic clock. In *China Satellite Navigation Conference (CSNC 2022) Proceedings*, pages 403–414, Singapore, 2022. Springer Nature Singapore.
- [6] DARPA. Atomic clock with enhanced stability (aces). <https://www.darpa.mil/program/atomic-clock-with-enhanced-stability>.
- [7] DARPA. Atomic clock with enhanced stability (aces) (archived). <https://www.darpa.mil/program/atomic-clock-with-enhanced-stability>.
- [8] DARPA. Darpa chip-scale atomic clocks aboard international space station. <https://phys.org/news/2012-03-darpa-chip-scale-atomic-clocks-aboard.html>.
- [9] DARPA. Micro-technology for positioning, navigation and timing - clocks (archived). <https://www.darpa.mil/program/micro-technology-for-positioning-navigation-and-timing/clocks>.
- [10] DARPA. Robust optical clock network (rockn). <https://www.darpa.mil/program/robust-optical-clock-network>.
- [11] Jonathan Hirschauer David R. Scherer, Bonnie L. Schmittberger. Current and future atomic clocks - roadmap and applications. <https://www.gps.gov/cgsic/meetings/2019/>.
- [12] John Elgin, Thomas Heavner, John Kitching, E.A. Donley, Jayson Denney, and Evan Salim. A cold-atom beam clock based on coherent population trapping. *Applied Physics Letters*, 115:033503, 07 2019.
- [13] GISGeography. How gps receivers work - trilateration vs triangulation. <https://gisgeography.com/trilateration-triangulation-gps/>.
- [14] Thai M. Hoang, Sang K. Chung, Thanh Le, John D. Prestage, Lin Yi, Robert I. Tjoelker, and Nan Yu. Performance of micro mercury trapped ion clock. In *2019 Joint Conference of the IEEE International Frequency Control Symposium and European Frequency and Time Forum (EFTF/IFC)*, pages 1–2, 2019.
- [15] Changhui Jiang, Shuai Chen, Yuwei Chen, and Yuming Bo. Research on a chip scale atomic clock driven gnss/sins deeply coupled navigation system for augmented performance. *IET Radar, Sonar & Navigation*, 13(2):326–331, 2019.

- [16] FairfieldNodal Inc. John Smythe. A nodal approach. <https://www.hartenergy.com/ep/exclusives/nodal-approach-176191>.
- [17] John Keller. Northrop to build electronic warfare (ew) rf jammers to protect warfighters from improvised explosives. <https://www.militaryaerospace.com/rf-analog/article/14196810/electronic-warfare-ew-rf-jammers-improvised-explosives>.
- [18] John Kitching. Time for a better receiver: Chip-scale atomic frequency references. (18), 2007-11-01 2007.
- [19] John Kitching. Chip-scale atomic devices. *Applied Physics Reviews*, 5(3):031302, 08 2018.
- [20] Svenja Knappe. *Emerging Topics MEMS Atomic Clocks*. Elsevier (Netherlands), Nov 2007.
- [21] Jet Propulsion Laboratory. Nasa activates deep space atomic clock. <https://www.jpl.nasa.gov/news/nasa-activates-deep-space-atomic-clock>.
- [22] X. Liu, V. I. Yudin, A. V. Taichenachev, J. Kitching, and E. A. Donley. High contrast dark resonances in a cold-atom clock probed with counterpropagating circularly polarized beams. *Applied Physics Letters*, 111(22):224102, 11 2017.
- [23] Bonnie L. Schmittberger Marlow and David R. Scherer. A review of commercial and emerging atomic frequency standards. *IEEE Transactions on Ultrasonics, Ferroelectrics, and Frequency Control*, 68(6):2007–2022, 2021.
- [24] Vincent Maurice, Zachary L. Newman, Susannah Dickerson, Morgan Rivers, James Hsiao, Phillip Greene, Mark Mescher, John Kitching, Matthew T. Hummon, and Cort Johnson. Miniaturized optical frequency reference for next-generation portable optical clocks. *Opt. Express*, 28(17):24708–24720, Aug 2020.
- [25] Mets501. Lambda-type system. https://commons.wikimedia.org/wiki/File:Lambda-type_system.pdf, 2012.
- [26] Microchip. Microchip technology inc. (website). <https://www.microsemi.com/>.
- [27] Izaak Neutelings. Beating waves. https://tikz.net/waves_beat/.
- [28] Zachary L. Newman, Vincent Maurice, Tara Drake, Jordan R. Stone, Travis C. Briles, Daryl T. Spencer, Connor Fredrick, Qing Li, Daron Westly, B. R. Ilic, Boqiang Shen, Myoung-Gyun Suh, Ki Youl Yang, Cort Johnson, David M. S. Johnson, Leo Hollberg, Kerry J. Vahala, Kartik Srinivasan, Scott A. Diddams, John Kitching, Scott B. Papp, and Matthew T. Hummon. Architecture for the photonic integration of an optical atomic clock. *Optica*, 6(5):680–685, May 2019.
- [29] NIST. Time and frequency from a to z. <https://www.nist.gov/pml/time-and-frequency-division/popular-links/time-frequency-z>.
- [30] Ajaykumar Patil. Vertical-cavity surface-emitting lasers market: Analysis of top manufacturers and their contributions. <https://medium.com/@ajaykumarpmr/vertical-cavity-surface-emitting-lasers-market-analysis-of-top-manufacturers-and-th>
- [31] PEOIEWS. Dagr. <https://www.flickr.com/photos/69349609@N02/6326407470>.
- [32] Nuclear Power. Nuclear power (website). <https://www.nuclear-power.com/>.

- [33] K. Ravi, Seunghyun Lee, Arijit Sharma, G. Werth, and S. A. Rangwala. Cooling and stabilization by collisions in a mixed ion–atom system. *Nature Communications*, 3(1):1126, Oct 2012.
- [34] Peter Schwindt, Y-Y Jau, Heather Partner, Darwin Serkland, Aaron Ison, Andrew McCants, Edward Winrow, John Prestage, J. Kellogg, Nan Yu, C. Boschen, Igor Kosvin, David Mailloux, David Scherer, Craig Nelson, Archita Hati, and David Howe. Miniature trapped-ion frequency standard with 171yb+. pages 752–757, 06 2015.
- [35] Peter D. D. Schwindt, Yuan-Yu Jau, Heather Partner, Adrian Casias, Adrian R. Wagner, Matthew Moorman, Ronald P. Manginell, James R. Kellogg, and John D. Prestage. A highly miniaturized vacuum package for a trapped ion atomic clock. *Review of Scientific Instruments*, 87(5):053112, 05 2016.
- [36] Petro Shine. Seismic methods. <https://petroshine.com/seismic-methods>.
- [37] Daniel A. Steck. Alkali d line data. <https://steck.us/alkalidata/>.
- [38] Martino Travagnin. Chip-scale atomic clocks: Physics, technologies, and applications. (KJ-NA-30790-EN-N (online)), 2021.
- [39] Wikipedia contributors. Dark state — Wikipedia, the free encyclopedia. https://en.wikipedia.org/w/index.php?title=Dark_state&oldid=1159294991, 2023. Online; accessed 19-March-2024.

A Atomic clock extensive comparison

Vendor	Product	Type	ADEV (1 s)	\mathcal{L} (10 Hz)	Aging (month)	Retrace	Tmin (°C)	Tmax (°C)	Tempco	Power (W)	Weight (kg)	Size (cm ³)
Muquans	MuC10ck	cold Rb	3,00E-13	-151						200,00	135,000	682000
T4Science	iMaser-3000	Maser	6,00E-14	-136	6,00E-15					100,00	100,000	436800
Microsemi	MHM 2020	Maser	8,00E-14	-138	9,00E-15					75,00	246,000	374072
Vremya	VCH-1003M	Maser	6,00E-14	-135	9,00E-15					100,00	100,000	305525
T4Science	pHMaster	PHM	5,00E-13	-130	6,00E-14					90,00	33,000	49820
Chengdu Spaceon	TA1000	OPC	1,20E-11	-125						100,00	40,000	48266
Spectradynamics	c-Rb	cold Rb	5,00E-13	-138						75,00	30,500	39806
Microsemi	5071A	CBT	5,00E-12	-130		0	55			50,00	30,000	29700
Oscilloquartz	OSA 3235B Cs	CBT	1,20E-11	-120						60,00	15,000	23021
Microsemi	cslll 4310B	CBT	1,20E-11	-130		0	50			30,00	13,500	16544
FEI	FEI RAFS	Space Rb	6,00E-13	-138	9,00E-13	5,00E-12	-4	25		39,00	7,500	4902
Spectratime	iSpace RAFS	Space Rb	3,00E-12	-120	8,30E-12		-5	10		35,00	3,400	3224
Excelitas	RAFS	space Rb	2,00E-12	-105	3,00E-12	5,00E-12	-20	45		39,00	6,350	1645
FEI	FE-5669	Rb	6,00E-12	-140	1,00E-11	2,00E-11	-20	60	5,00E-11	20,00	1,690	669
Microchip	XPRO (low drift)	Rb	1,00E-11	-90	1,00E-11	3,00E-11	-25	70	6,00E-10	13,00	0,500	455
Spectratime	miniRAFS	Rb	1,00E-11	-84	3,00E-11		-15	55		10,00	0,450	388
IQD	IQRB-2	Rb	2,00E-12	-138	4,00E-11	2,00E-11				6,00	0,220	230
Spectratime	LP Rb	Rb	1,00E-11	-100	3,00E-11	5,00E-11	-25	55	2,00E-10	10,00	0,290	216
SRS	PRS10	Rb	2,00E-11	-130	5,00E-11	5,00E-11	-20	65	2,00E-10	14,40	0,600	155
Accubeat	AR133A	Rb	5,00E-12	-116	1,00E-11	5,00E-11	-20	65	1,00E-10	8,25	0,295	146
IQD	IQRB-1	Rb	5,00E-11	-95	5,00E-11	2,00E-11	0	50	5,00E-10	6,00	0,105	66
Chengdu Spaceon	XHTF1031 Rb	CPT	5,00E-11	-95	5,00E-11		-30	65	2,00E-10	6,00	0,200	65
Spectratime	mRO-50 (EAS)	CSAC	4,00E-11	-76	1,50E-10	1,00E-10	-10	65	4,00E-10	0,36	0,075	50
Microsemi	SA55 MAC	CPT	3,00E-11	-87	5,00E-11	5,00E-11	-10	75	5,00E-11	6,30	0,100	46
Accubeat	NAC	CSAC	2,00E-10	-86	3,00E-10		-20	65	2,00E-09	1,20	0,075	32
Chengdu Spaceon	CPT	CSAC	2,00E-10	-90	9,00E-10	5,00E-11	-45	70	5,00E-10	1,60	0,045	24
Teledyne	TCSAC	CSAC	3,00E-10	-85	3,00E-10	3,00E-10	-10	60	1,00E-09	0,18	0,042	23
Microsemi	SA45.s	CSAC	3,00E-10	-70	9,00E-10	5,00E-10	-10	70	1,00E-09	0,12	0,035	17
Microsemi	SA65	CSAC	3,00E-10	-64	9,00E-10	5,00E-10	-40	80	3,00E-10	0,12	0,035	16

Table 1: Performance parameter for some of the most common atomic clock. Source [23].

B Chip-Scale Atomic Clocks comparison

Manufacturer/Model	Country	ADEV (1 s)	Power (W)	Size (cm ³)
Jackson Labs CSAC GPSDO	US	1E-10	1,4	85
Seiko Epson A06860LAN	JP	3E-11	3,0	75
Precision Test Systems RFS2	UK	3E-11	6,0	65
Quartzlock El O-MRX	UK	5E-11	6,0	65
Microsemi MAC SA.3Xm	US	3E-11	5,0	50
Orolia Spectratime mRO-50	CH/FR	4E-11	0,5	50
Chengdu Spaceon XHTF1031	China	5E-11	6,0	50
Microsemi MAC SA.5X	US	3E-11	6,3	47
Accubeat NAC1	Israel	2E-10	1,2	32
IQD ICPT-1	UK	9E-11	1,7	25
Chengdu Spaceon XHTF1040	China	3E-10	1,6	24
Teledyne TCSAC	US	3E-10	0,2	23
Microsemi SA45.s	US	3E-10	0,1	17
Chengdu Spaceon XHTF1045	China	3E-10	0,3	17

Table 2: Key parameters of the most common CSACs. Source [38].

C Rubidium energy levels

Here follows a more comprehensive description of the energy levels of ^{87}Rb isotopes, as shown in Figure 26. The hyperfine structure of the $5^2\text{S}_{1/2}$ and $5^2\text{P}_{1/2}$ states is due to the interaction between the nuclear magnetic moment and the electron magnetic moment. The hyperfine structure of the $5^2\text{P}_{3/2}$ state is due to the interaction between the nuclear magnetic moment and the total angular momentum of the electron. The $5^2\text{S}_{1/2}$ state has two hyperfine levels, $F = 1$ and $F = 2$, separated by $\Delta E_{hfs} = 6.834682610904(10)\text{GHz}$.

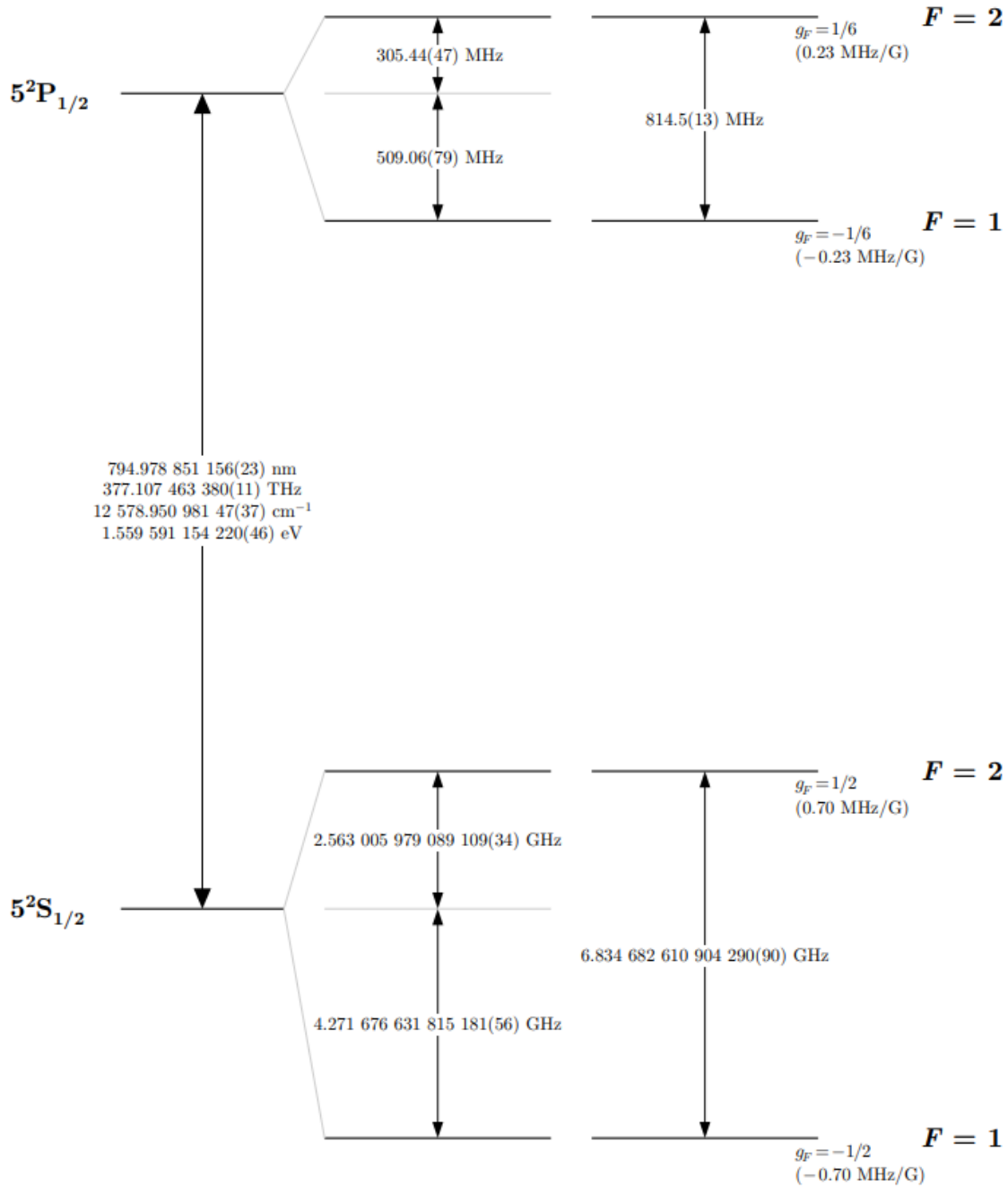


Figure 26: Energy levels of ^{87}Rb . Source [37].

D Cesium energy levels

Here follows a more comprehensive description of the energy levels of ^{133}Cs isotopes, as shown in Figure 27. The hyperfine structure of the $6^2S_{1/2}$ and $6^2P_{1/2}$ states is due to the interaction between the nuclear magnetic moment and the electron magnetic moment. The hyperfine structure of the $6^2P_{3/2}$ state is due to the interaction between the nuclear magnetic moment and the total angular momentum of the electron. The $6^2S_{1/2}$ state has two hyperfine levels, $F = 3$ and $F = 4$, separated by $\Delta E_{hfs} = 9.192631770(10)$ GHz.

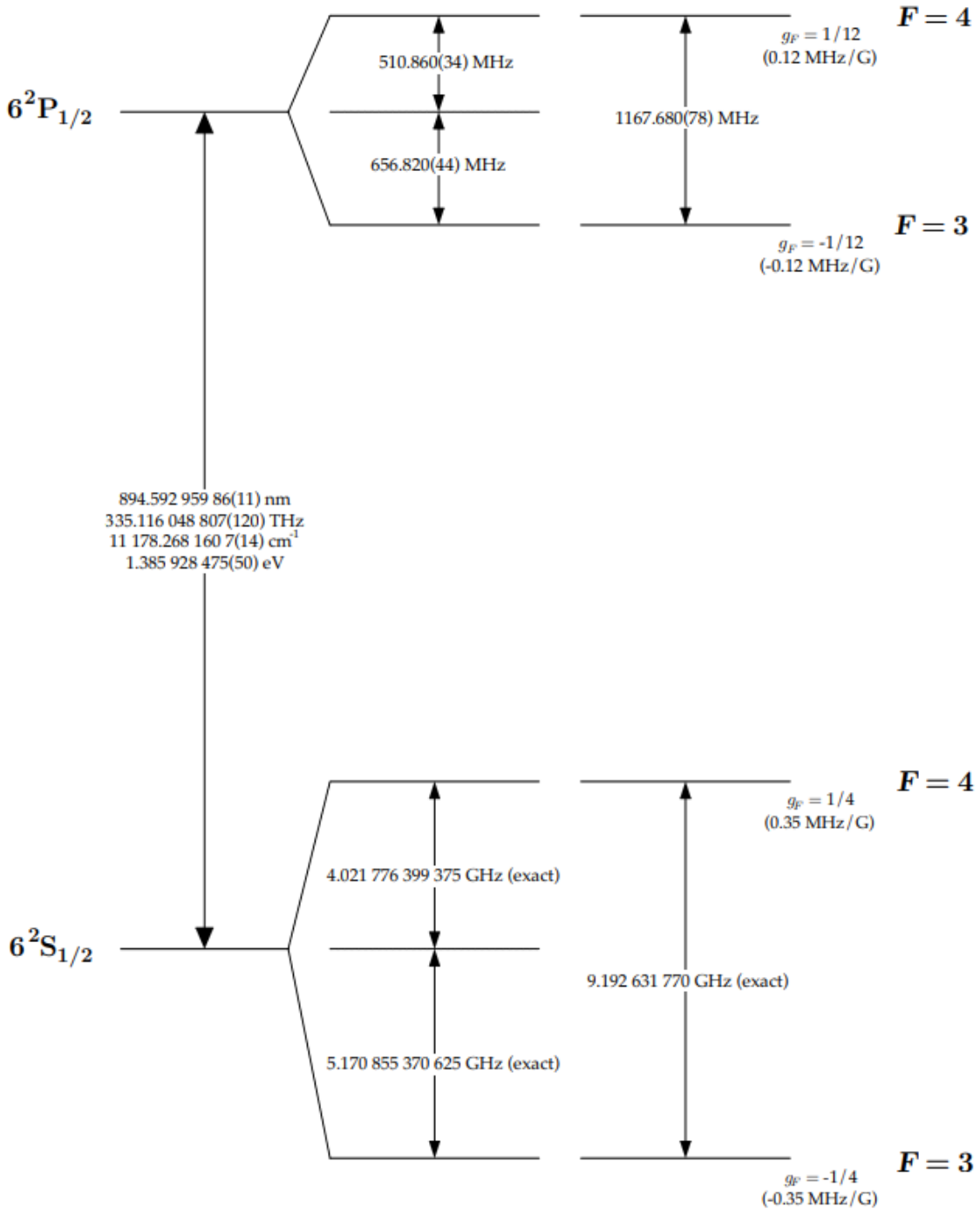


Figure 27: Energy levels of ^{87}Rb . Source [37].